Computers and Concrete, *Vol. 19, No. 1 (2017) 087-098*
DOI: https://doi.org/10.12989/cac.2017.19.1.087

Crashworthiness analysis on existing RC parapets rehabilitated with UHPCC

Jinkai Qiu[1,2a], Xiang-guo Wu[*1,2] and Qiong Hu[1,2b]

[1]*Key Lab of Structures Dynamic Behavior and Control of the Ministry of Education, Harbin Institute of Technology, Harbin, 150090, China*
[2]*School of Civil Engineering, Harbin Institute of Technology, Harbin, 150090, China*

(Received July 11, 2015, Revised October 3, 2016, Accepted October 28, 2016)

Abstract. In recent year, the coat layer drops and the rebar rust of bridge parapets, which caused the structural performance degradation. In order to achieve the comprehensive rehabilitation, ultra high performance cementitious composites is proposed to existing RC parapet rehabilitation. The influence factors of UHPCC rehabilitation includes two parts, i.e., internal factors related with material, such as UHPCC layer thickness, corrosion ratio of rebars, fiber volume fraction, and external factors related with the load, such as impact speeds, impact angles, vehicle mass. The influence of the factors was analyzed in this paper based on the nonlinear finite element. The analysis results of the maximum dynamic deformation and the peak impact load of parapets revealed the influence of the internal factors and the external factors on anti-collision performance and degree degradation. This research may provide a reference for the comprehensive multifunctional rehabilitation of existing bridge parapets.

Keywords: parapets; rehabilitation; UHPCC; impact load; deformation

1. Introduction

The parapet is one of the major forms of the anti-collision guardrails in bridges. The parapet needs to meet not only the aesthetic requirements, but also the anti-collision design level. However, in recent years, the coat layer on bridge parapets drops and the rebar rusts because of the insufficient durability, etc., which is still widespread now. And it caused the further degradation of durability and structural performance. Comprehensive rehabilitation including the durability and the anti-collision performance has important engineering significances for the existing parapets.

As a new generation of high-performance cementitious composite materials (Dugat *et al*. 1996), ultra high performance cementitious composites (UHPCC) has excellent performances including mechanics and durability. Strengthening and rehabilitation of existing concrete structures is one of the important engineering applications for UHPCC.

Recently, UHPCC is applied to durability rehabilitation and load-carrying capacity strengthening of existing RC structures, such as the bridge deck (Brühwiler and Denarie. 2008), prestressed concrete members (Habel and Gauvreau 2009), the pavement (Schmidt *et al*. 2008), beams and slabs (Bastien and Bruehwiler 2014), and the rehabilitation of reinforced concrete members (Prem *et al*. 2015), etc. The composite structure including the UHPCC rehabilitation layer and existing structure members makes the rehabilitation of UHPCC become the comprehensive rehabilitation which contains the rehabilitation of the durability and the load-carrying capacity. In recent years, some research work were carried out on the composite behavior of UHPCC and normal concrete (Wu *et al*. 2014, Wu *et al*. 2012, Wu *et al*. 2013, Bruhwilerand Denarie 2013a, b, Oesterlee *et al*. 2007, Moreillon and Menétrey 2013). Brühwiler (2013a, b) studied flexural and shear behavior of UHPCC-RC composite beams, and applied it to the engineering rehabilitation of bridge pavement and bridge parapets. In addition, the mechanical properties of the bridge reinforced concrete parapets with a UHPCC overlay were studied (Charron *et al*. 2011, Duchesneau *et al.* 2011). However, the research on UHPCC rehabilitation of existing bridge parapets, especially its anti-collision performance, is relatively few.

In this paper, the effect of UHPCC rehabilitation on the anti-collision performance of parapets is studied. Finite element model is established and it is verified previously by the composite slab impact test results of Habel and Gauvreau (Habel and Gauvreau 2009). The influence factors of UHPCC rehabilitation are divided into two parts, i.e., internal factors related with material, such as UHPCC layer thickness, corrosion ratio of rebars, fiber volume fraction, and external factors related with the load, such as impact speeds, impact angles, vehicle mass. According to the analysis results, the influence of internal factors and external factors on the anti-collision performance and the anti-collision level is revealed including the maximum

∗Corresponding author, Professor
E-mail: wuxiangguo@hit.edu.cn
[a]Ph.D. Student, E-mail: qiukai.2008@163.com
[b]Associate Professor, E-mail: huqiong@hit.edu.cn

ISSN: 1598-8198 (Print), 1598-818X (Online)

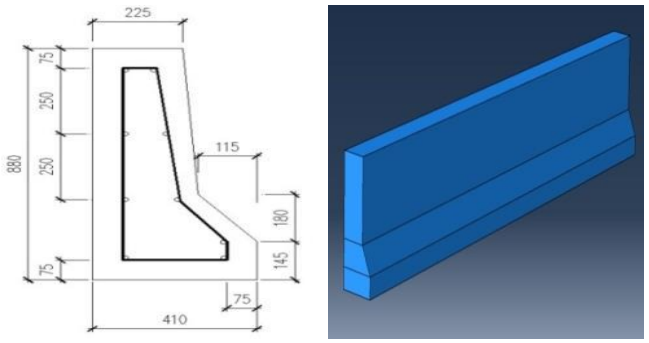

(a) Section size (b) Finite element model

Fig. 1 Dimensions and model of the original parapet

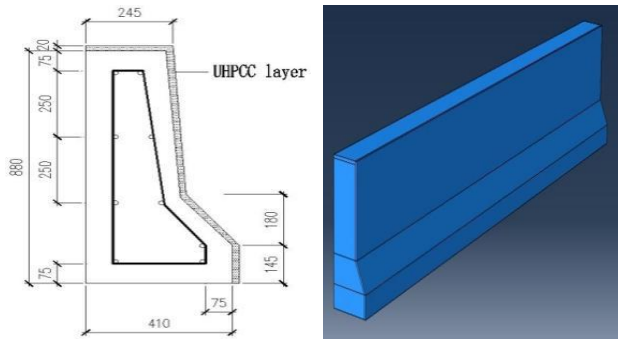

(a) Section size (b) Finite element model

Fig. 2 Dimensions and model of the rehabilitated parapet with 20 mm UHPCC layer

Table 1 Division of the anti-collision level

Anti-collision level	Impact conditions			Impact acceleration (m/s^2)	Impact energy (kJ)
	Impact speed (km/h)	Vehicle mass (t)	Impact angle (°)		
B	100	1.5	20	≤200	
	40	10	20		70
A, Am	100	1.5	20	≤200	
	60	10	20		160
SB, SBm	100	1.5	20	≤200	
	80	10	20		280
SA, SAm	100	1.5	20	≤200	
	80	14	20		400
SS	100	1.5	20	≤200	
	80	18	20		520

dynamic deformation and the peak impact load of parapets. The research may provide a reference for the comprehensive rehabilitation of bridge parapets based on UHPCC.

2. Finite element modeling of vehicle-parapets

2.1 The parapet model

New Jersey parapets (NJ type) (National Standard of the P.R.C.1994) are adopted in this paper. The section size and finite element model of the original parapet are shown in Fig. 1.

The corresponding section dimensions and the model of rehabilitated parapet are shown in Fig. 2. The parapet generally sets a temperature seam along the longitudinal direction every 6 m. The lower surface of the parapet and the corresponding upper surface of the bridge deck are connected by the "Tie" model, and a rigid connection is applied to the bottom surface of the bridge deck.

2.2 Division of anti-collision level

The anti-collision level division of parapets (Industry recommended standard of the R.P.C, 2006) is shown in Table 1.

Table 2 Partial material parameters of d_c

$\varepsilon\times10^{-6}$	899	1099	1299	1499	1599	1799	1999
x	0.53	0.65	0.77	0.89	0.95	1.07	1.18
d_c	0.09	0.15	0.22	0.30	0.33	0.41	0.49

Table 3 Partial material parameters of d_t

$\varepsilon\times10^{-6}$	128	139	189	242	279	309	359
x	1.03	1.12	1.52	1.95	2.25	2.49	2.90
d_t	0.17	0.29	0.68	0.83	0.88	0.91	0.93

Table 1.

According to the impact energy (National Standard of the R.P.C, 1994), the anti-collision levels of parapets are divided. The impact energy E of vertical action on the parapets can be determined by

$$E = 9810 \cdot \frac{1}{2g} W \cdot V^2 \sin^2 \theta \tag{1}$$

Where g is gravity acceleration (9.81m/s^2); W is the Vehicle mass (t); V is the impact speed (m/s); θ is the impact angle (°).

2.3 Material model

The uniaxial stress-strain relationship of concrete (National Standard of the P.R.C. 2010) is shown in Fig. 3(a). The concrete with standard compressive strength ($f_{c,r}$) 33 MPa and the tensile strength ($f_{t,r}$) 3.3 MPa is assumed in the parapets, in which the corresponding strains $\varepsilon_{c,r}$ and ε_{cu} are equal to 1688×10^{-6} and 3679×10^{-6}, and strain $\varepsilon_{t,r}$ is equal to 124×10^{-6}. And E-modulus is 3.09×10^4 N/mm^2. The Poisson's ratio was 0.2.

The relationship of uniaxial compressive and tensile stress-strain can be determined by

$$\sigma=(1-d_c)E_c\varepsilon \tag{2}$$

And

$$\sigma=(1-d_t)E_c\varepsilon \tag{3}$$

In which, d_c is the evolution parameters of uniaxial compressive damage. E_c is the modulus of elasticity. d_t is

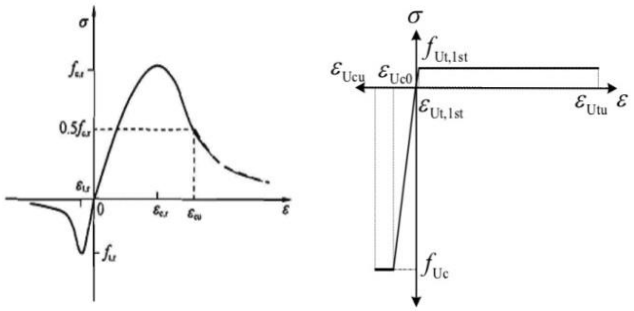

(a) Normal concrete (b) UHPCC

Fig. 3 Uniaxial stress-strain relation of the materials

the evolution parameters of uniaxial tensile damage. The two damage parameters can be calculated from Eqs. (4) and (5) which can be referenced from (National Standard of the P.R.C. 2010).

$$d_c=\begin{cases}1-\dfrac{\rho_c n}{n-1+x^n} & x\le 1\\ 1-\dfrac{\rho_c}{\alpha_c(x-1)^2+x} & x>1\end{cases} \tag{4}$$

Here, $\rho_c=\dfrac{f_{c,r}}{E_c\varepsilon_{c,r}}$, $n=\dfrac{E_c\varepsilon_{c,r}}{E_c\varepsilon_{c,r}-f_{c,r}}$, and $x=\dfrac{\varepsilon}{\varepsilon_{c,r}}$.

$$d_t=\begin{cases}1-\rho_t\left[1.2-0.2x^5\right] & x\le 1\\ 1-\dfrac{\rho_t}{\alpha_t(x-1)^{1.7}+x} & x>1\end{cases} \tag{5}$$

In which, $\rho_c=\dfrac{f_{t,r}}{E_c\varepsilon_{t,r}}$ and $x=\dfrac{\varepsilon}{\varepsilon_{t,r}}$.

The partial values of d_c and d_t are shown in Table 2 and Table 3.

The steel rebar of the parapet were vertical steel bars and longitudinal bars. HRB335 of hot rolled steel bar was adopted here. Section area of stirrups and longitudinal bars are 70.85 mm^2 and 200.96 mm^2, respectively. The stirrup spacing is 150 mm. Elasto-plastic model is used for steel bar. The standard yield strength and standard ultimate limit strength are equal to 335 MPa and 455 MPa. E-modulus is equal to 2.00×10^5 N/mm^2. Corresponding yielding strain and ultimate strain are equal to 1675 $\mu\varepsilon$ and 75000 $\mu\varepsilon$, respectively.

The ideal Elastic-plastic model (Benjamin 2006) is used for UHPCC, which omitted its strain hardening range, as shown in Fig. 3(b). The mixture ratio of UHPCC considering in this study is shown in Table 4, in which steel fiber volume fraction is considered as a design variable including 0.0%, 1%, and 2%. Material Poisson's ratio is equal to 0.18, and E-modulus is equal to 50 GPa. The material model parameters are based on the test results of Yang (Yang 2006), as are shown in Table 5.

The Poisson's ratio effect on the peak impact force and the ultimate maximum dynamic deformation is low and a unified value of 0.18 is selected for Poisson's ratio in the analysis. The elastic modulus test, were given 52.84 GPa, 53.25 GPa, 56.85 GPa, but also has no effect on the peak value of impact force and the maximum dynamic deformation. A unified value of 50 GPa is selected for this parameter. According to relationship between the cubic compressive strength and prism compressive strength of UHPC (Wang *et al*. 2013), f_c=0.874f_{cu}, prism compressive strength is considered as the compression strength and cracking strength is selected as the constitutive model tension strength as shown in Fig. 3. The variation of the mass density is small and it is not the main factor that affects the impact force and the maximum dynamic deformation. So a unified value of 2465 kg/m^3 is selected for the analysis. Corresponding model parameter values of UHPCC material for the following analysis are listed in Table 6.

Table 4 Mixture ratio of UHPCC (kg/m^3)

No.	Cement	Silica fume	Fine sand	Water	Fiber volume fraction (%)	Super plasticizer
1	706	160	1249	122	0	74
2	706	160	1329	122	80	74
3	706	160	1249	122	160	74

Table 5 Material experimental results of UHPCC

No.	Mass density (kg/m3)	Compressive strength (MPa)	Tensile strength (MPa)	Initial Cracking strength (MPa)	Tensile ultimate strain εUtu (×10-6)	Elastic modulus (GPa)
1	2463	97.65	5.90	3	157	52.84
2	2465	124.82	10.25	6	217	53.25
3	2465	159.40	14.57	9	325	56.85

Table 6 Model parameters value of UHPCC

Fiber fraction (%)	Mass density (kg/m^3)	Poisson's ratio	Compressive strength (MPa)	Tensile strength (MPa)	Modulus of elasticity (GPa)
0	2465	0.18	88	3	50
1	2465	0.18	110	6	50
2	2465	0.18	140	9	50

2.4 Model verification

Recently, Habel and Gauvreau (2009) carried out an impact test of RC composite slab with a UHPFRC overlay. The test specimen is a cantilever slab, and its geometry and load characters are very close with parapet rehabilitated with UHPCC layer, Therefore, the test specimens were modeled firstly. And the verified FEM model will be used in the following parapet analysis. This FEM model was established in the previous research. The results of the Habel test and the verification were briefly introduced here.

The size of the specimen was 250 mm×200 mm×3600 mm. The geometry size and the detail of the reinforcement are shown in Fig. 4(a) and (b). In this paper on the basis of ensuring the accuracy, in order to improve the computational efficiency, "C3D8R" element (8 nodes with 6 sides reduced integral element) is used to simulate ordinary concrete and UHPCC and "T3D2" element (3 dimensional 2 node truss element) is used to simulate

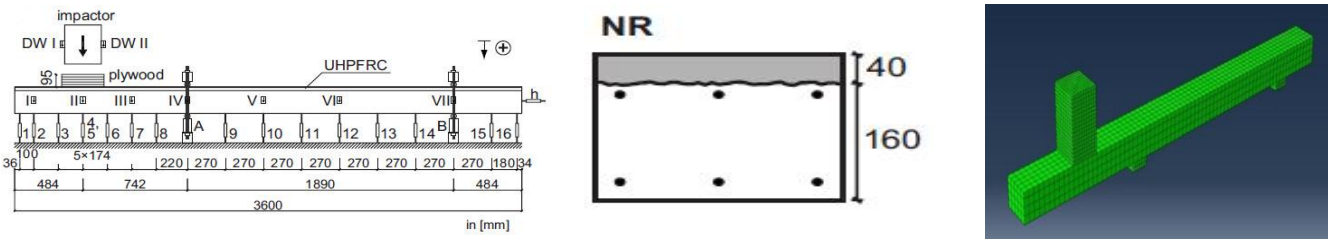

(a) Geometric dimensions (b) Reinforcement (c) Finite element model

Fig. 4 Geometric dimensions, reinforcement and model of the slab strip

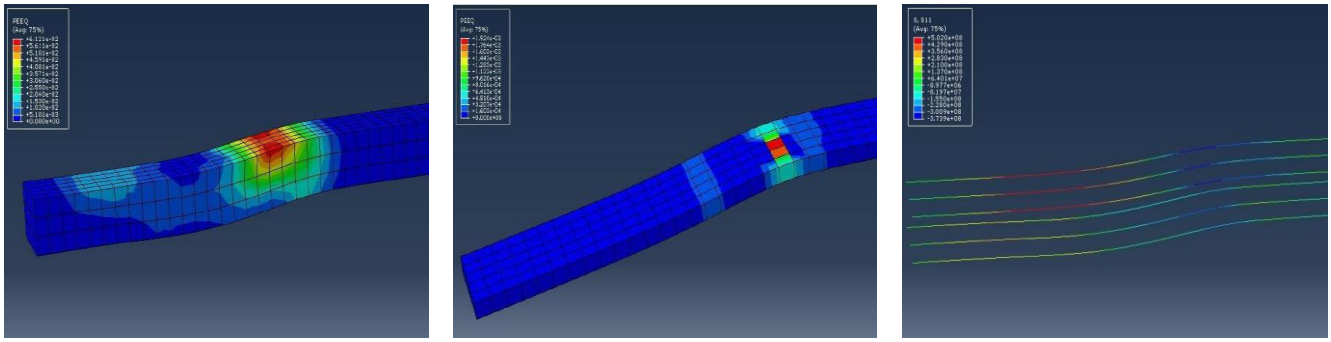

(a) NC part (b) UHPCC part (c) Reinforcement bar

Fig. 5 Simulation results

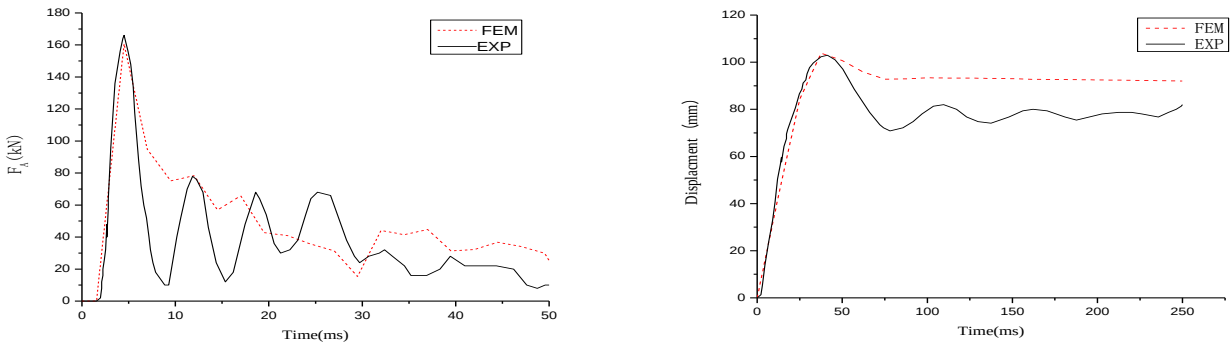

(a) Impact load (b) Displacement

Fig. 6 Comparison of test values and simulation values

reinforcement. UHPCC layer is divided along its thickness direction with the size of 40 mm, and is divided in its length direction with the size of 50 mm. NC part is divided into 3 sections along its thickness direction. Along its length direction, NC is divided with the size of 50 mm. In this paper, the contact between NC and UHPC is defined as the tangential rough contact without slip and normal hard contact. And the contact algorithm of "universal contact" is adopted which are in good agreement with the test results. The finite element model is shown in Fig. 4(c).

The reinforcing bars cross section is 100 mm^2. Coupon tests indicated the yield strength of 470 MPa with a well-defined yield plateau and an ultimate strength of 750 MPa. The compressive strength, tested on three cylinders (diameter 100 mm), was 128 MPa at 28 days and 131 MPa at the age of testing of the composite slab strips (100 days).

The uniaxial tensile strength was 11 MPa at a deformation of 0.15% at 28 days. It had a compressive strength of 33 MPa after 28 days and 37 MPa at the time of testing of the composite slab strips (250 days).

The UHPC model has been established and participated in the model calculation. The analyzed results of NC part, UHPC part and reinforcement bar are show in Fig. 5(a), (b) and (c), respectively.

The impact load test values are compared with the simulated values as shown in Fig. 6. The results show that rise and fall of the impact load test values are smoother, impact time of the test is longer than that of the simulation, but overall, simulation values are in good agreement with the test values. According to Fig. 6(a), the greatest impact load test value and simulation value at the support F_A of test specimen is close, respectively is 160.5 kN and 166 kN, and the impact load shock wave and the peak of numerical simulation are relatively close.

According to Fig. 6(b), the peak value of displacement simulation and the experimental result of composite slab subjected to impact are in good agreement. But the simulation results after the peak value is relatively

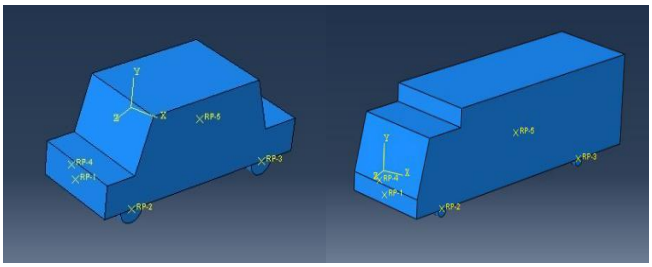

(a) Car (b) Large truck

Fig. 7 Finite element model of the vehicle

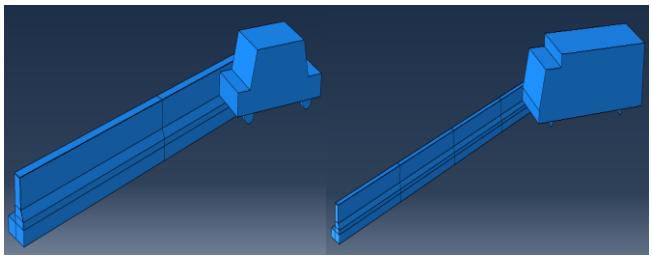

(a) Car (b) Large truck

Fig. 8 Finite element model of oblique collision

smoother. It differed greatly from the experimental results. The reasons of the difference between the test value and the simulation value are as follows.

(1) The influence of the secondary impact on the displacement is not considered in the simulation, so the fluctuation and the shock phenomenon of the test results are not reflected.

(2) Drop hammer is supposed to be rigid with certain approximation. In simulation, in order to simplify the calculation, drop hammer is seen as a rigid body. And drop hammer is deformed from the test results. We can see the obvious tremor by high speed camera. It can be presumed drop hammer itself consumed some energy in the impact process.

2.5 Vehicle model

In this paper, the vehicle model is divided into cars and large trucks (Tai 2010) according to the impact mass. The structure size of the car is 3.6 m length, 1.4 m wide, 1.5 m high, and the mass of the car is respectively 1.5 t. The structure size of the large trucks is 10.5 m long, 2.5 m wide, 2.7 m high. In order to carry out vehicle parameters analysis of different mass, according to the China national standard "The Evaluation Specification for Highway Safety Barriers" (JTG / F83-01-2004) (National Standard of the P.R.C. 2004). The truck's mass is 10 t, 14 t, 18 t, respectively. The vehicle total mass is controlled by material quality density. To analysis ultimate impact resistance of parapets conservatively, the vehicle models are considered as the rigid body, and the simplified model of the vehicle was shown in Fig. 7.

3. Influence factors consideration

3.1 Internal factors

Table 7 Analysis specimen of original corroded RC parapets

Name	Corrosion ratio of rebars (%)	Thickness of the rehabilitation layer (mm)
CR0-UT0	0	0
CR5-UT0	5	0
CR10-UT0	10	0
CR15-UT0	15	0
CR20-UT0	20	0
CR25-UT0	25	0
CR30-UT0	30	0

Table 8 Analysis specimen of rehabilitated parapets

Name	Thickness of the rehabilitation layer (mm)	Fiber volume fraction (%)
UT20-0	20	0
UT30-0	30	0
UT40-0	40	0
UT20-1	20	1
UT30-1	30	1
UT40-1	40	1
UT20-2	20	2
UT30-2	30	2
UT40-2	40	2

Table 9 External factor design

Name	Vehicle mass (t)	Impact speeds (km/h)	Impact angles (°)
M1V2θ1	1.5	80	15
M1V1θ2	1.5	100	20
M1V2θ2	1.5	80	20
M1V2θ3	1.5	80	25
M1V3θ2	1.5	60	20
M2V2θ1	10	60	15
M2V2θ3	10	60	25
M2V2θ2	10	80	20
M2V3θ2	10	60	20
M3V2θ1	14	60	15
M3V2θ3	14	60	25
M3V3θ2	14	60	20
M4V2θ1	18	60	15
M4V3θ2	18	60	20
M4V2θ3	18	60	25

This section considers the effects of the parameters (the corrosion ratio of rebar, the thickness of UHPCC rehabilitation layer and fiber volume fraction) on anti-collision performance of the parapet through the vertical collision simulation process. The thickness of UHPCC rehabilitation layer is respectively 20 mm, 30 mm, 40mm. The corrosion rate of rebar is respectively 0%, 5%, 10%, 15%, 20%, 25%, 30%.The fiber volume fraction is respectively 0%, 1%, 2%. The number of the test specimen and the influence considerations are shown in Tables 7-8.

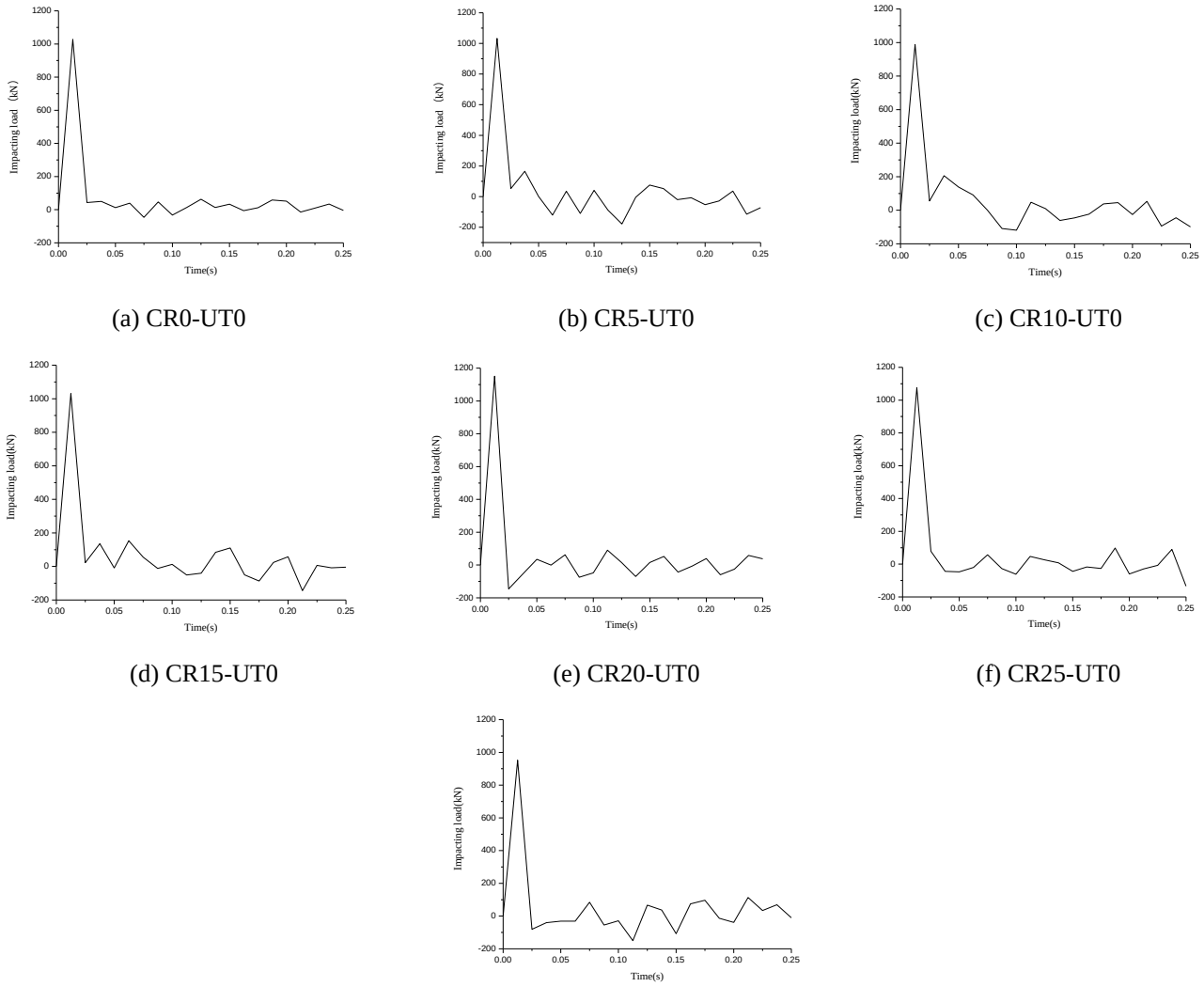

(a) CR0-UT0 (b) CR5-UT0 (c) CR10-UT0

(d) CR15-UT0 (e) CR20-UT0 (f) CR25-UT0

(g) CR30-UT0

Fig. 9 Impact load versus time curve of the simulation model

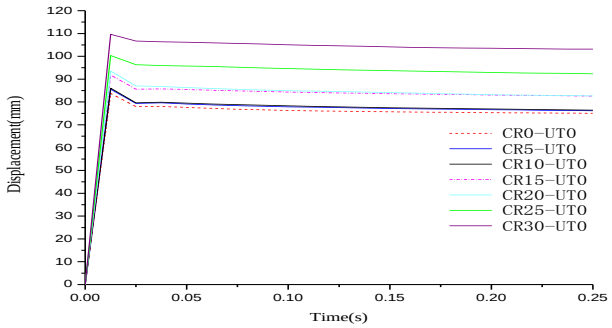

Fig. 10 Comparison among different models

In Table 7, the letter "CR" represented corrosion rate of rebars, subsequent number 0, 5, 10, 15, 20, 25, 30 means that corrosion rate is 0%, 5%, 10%, 15%, 20%, 25%, 30%, respectively. In Table 5, "UT" represents the thickness of UHPCC rehabilitation layer, subsequent number 0, 20, 30, 40, means that the thickness of UHPCC rehabilitation layer is 0 mm (the parapet was not rehabilitated), 20 mm, 30 mm, 40 mm, respectively.

3.2 External factors

In simulating the collision process, vehicle mass, impact speed and impact angle are respectively three important factors of the initial conditions of the collision. In this paper, the influence of the parameters (impact speeds, impact angles and vehicle mass) on the anti-collision performance including the impact load and the maximum dynamic deformation are analyzed. The models are shown in Fig. 8. The test specimen information is shown in Table 9.

In Table 8, the letter "M" represents the vehicle mass, subsequent number 1, 2, 3, 4 means that vehicle mass is 1.5 t, 10 t, 14 t, 18 t, respectively; "V" represented vehicle speed, subsequent number 1, 2, 3 means that the impact speed is 100 km/h, 80 km/h, 60 km/h, respectively; the letter "θ" represents the vehicle angle, subsequent number 1, 2, 3 means that the impact angles is 15°, 20°, 25°, respectively.

4. Results and analysis

Table 10 Numerical results of original RC parapets with varied corrosion rates

Name	Corrosion rate of rebars, η_s (%)	f_{ys} (MPa)	Peak impact load (kN)	Maximum dynamic deformation (mm)	Anti-collision level
CR0UT0	0	335	1028	83.7	B
CR5-UT0	5	313	1030	85.6	B
CR10-UT0	10	296	988	86.1	B
CR15-UT0	15	278	1030	91.8	B
CR20-UT0	20	261	1150	93.5	B
CR25-UT0	25	243	1076	100.4	B
CR30-UT0	30	226	952	109.6	B

4.1 Effect of the corrosion rate of rebars

Experiments results (Zhang 1995, Zhang 2006, Almusallam 2001, Wang 2003) show that with the increase of the corrosion rate of rebars, nominal yield strength, ultimate strength and ultimate elongation decreases, and yield platform shortened or even disappeared, but the modulus of elasticity didn't change obviously. The relationships between nominal yield strength and the corrosion rate of steel bars are follows (Zhang 1995)

$$f_{ys} = (0.986 - 1.038\eta_s) f_y \tag{6}$$

Where f_{ys} is the yield strength of corroded rebars; f_y is the original yield strength of the rebars; η_s is the corrosion rate of rebars (η_s>0).

According to the numerical results of the vehicle-parapet collision process, the peak impact load and the maximum dynamic deformation of the original parapet change with the change of the steel bar corrosion rate under the vertical impact of vehicle. The main numerical results are shown in Table 10.

According to the above simulation results, the impact load versus time curve and the displacement versus time curve for different steel corrosion rates are obtained, as shown in Figs. 9-10.

Analysis results of the impact load versus time curve show that the vertical impact of the vehicle on the parapet produces a greater impact load. With the increase of the steel bar corrosion rates, the impact load of the parapet doesn't show obvious regularity, but the corresponding maximum dynamic deformation increases gradually with the steel bar corrosion rate increasing. From Table 10, it can be found that when the rebar corrosion rate is less than 25%, the maximum dynamic deformation of anti-collision are less than 100 mm. The anti-collision performance is good and it could meet the requirements of specification (National Standard of the P.R.C. 2004). When the rebar corrosion rate is up to 25%, the maximum dynamic deformation is 100.4 mm. At this time it has reached the threshold value of maximum dynamic deformation which specification requires. When the rebar corrosion rate is 30%, the maximum dynamic deformation is 109.6 mm; apparently it doesn't meet the requirement of the anti-collision performance.

When the maximum dynamic deformation of concrete anti-collision wall is up to 100 mm under the vertical impact of the vehicle, the steel bar corrosion rate is defined as the threshold value of steel bar corrosion rate. In conclusion, when the steel bar corrosion rate reaches 25%, the anti-collision performance of the concrete anti-collision wall doesn't meet the requirement. Therefore, the threshold value of the steel bar corrosion rate is 25%.

Table 11 Numerical results of NC parapets for different UHPCC thickness

Name	Fiber volume fraction (%)	UT (mm)	Impact load (kN)	Deformation (mm)	Anti-collision level
T0-0	0	0	1076	100.4	B
T20-0		20	1097	74.01	B
T30-0		30	1160	66.2	B
T40-1		40	1192	58.5	B
T0-1	1	0	1076	100.4	B
T20-1		20	1159	64.4	B
T30-1		30	1215	55.3	B
T40-1		40	1246	46.9	B
T0-2	2	0	1076	100.4	B
T20-2		20	1209	57.04	B
T30-2		30	1244	48.56	B
T40-2		40	1260	43.04	B

4.2 Influence of UHPCC rehabilitation layer thickness

UHPCC is used to rehabilitate parapets which achieve the threshold value of steel bar corrosion rate. Through the vehicle collision, we can get peak impact load and the maximum dynamic deformation of parapets of different UHPCC rehabilitation layer thickness. The numerical results are shown in Table 11.

The above simulation results show that the impact load versus time curve and the displacement versus time curve for different UHPCC layer thickness are obtained, and as shown in Fig. 11 and Fig. 12.

According to Fig. 11, when the fiber volume fraction of UHPCC is 0%, 1%, 2%, with the increase of UHPCC rehabilitation layer thickness, the impact load increases gradually. But the growth rate is smaller. When the fiber volume fraction is 0%, the parapets of 20 mm, 30 mm, 40 mm thickness of UHPCC rehabilitation layer are compared to original parapets that are not rehabilitated by UHPCC and the impact load increases by 1.95%, 7.8%, 10%, respectively; when the fiber volume fraction is 1%, the parapets that used UHPCC 20 mm, 30 mm, 40 mm rehabilitation layer thickness under the vehicle impact are compared to the above original parapets, the impact load increases by 7.7%, 12.9%, 15.8%, respectively; when the fiber volume fraction is 2%, the impact load increases by 12.36%, 15.6%, 17.7%, respectively.

According to Fig. 12, with the increase of UHPCC

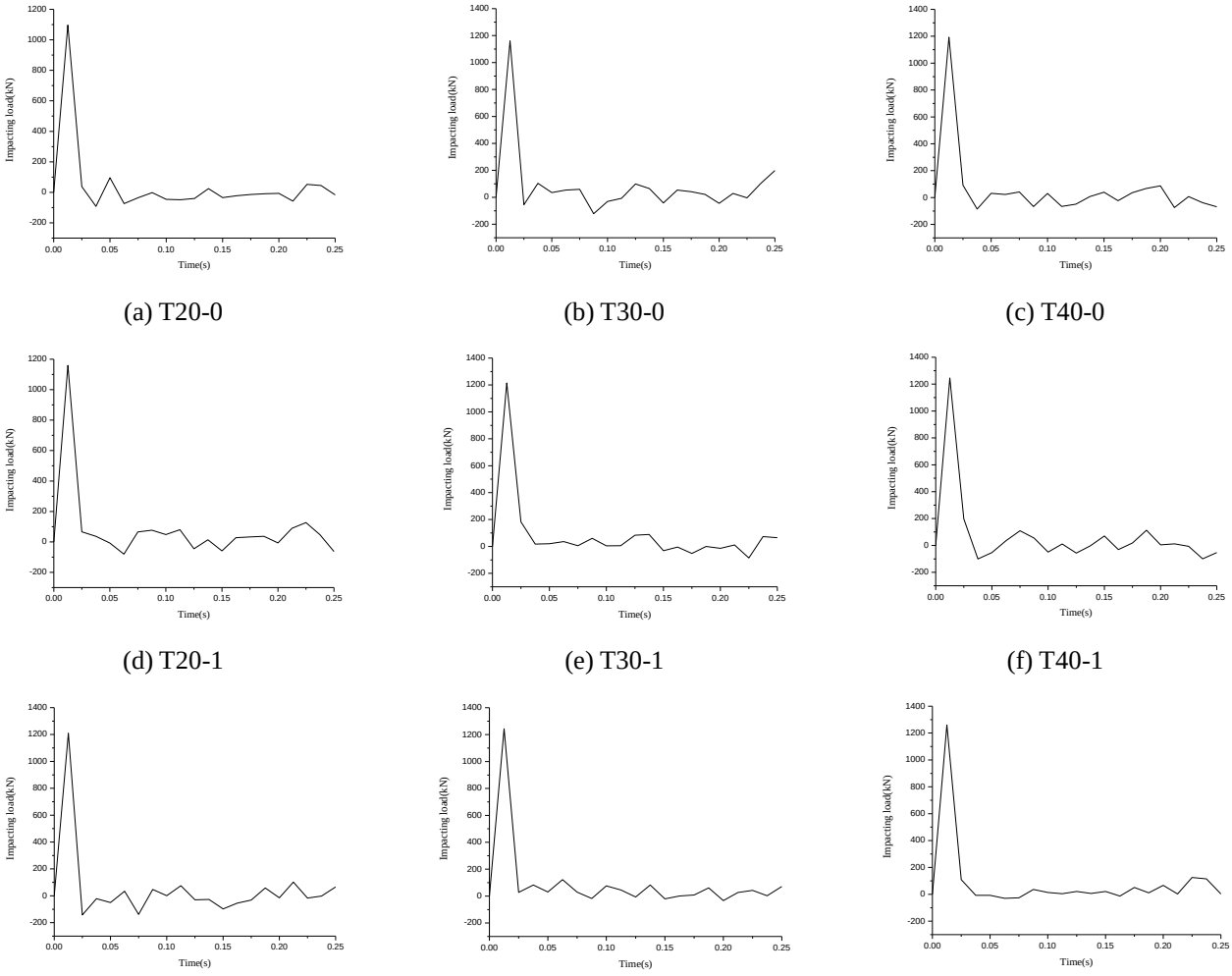

(a) T20-0 (b) T30-0 (c) T40-0

(d) T20-1 (e) T30-1 (f) T40-1

(g) T20-2 (h) T30-2 (i) T40-2

Fig. 11 Impact load versus time curve for different models

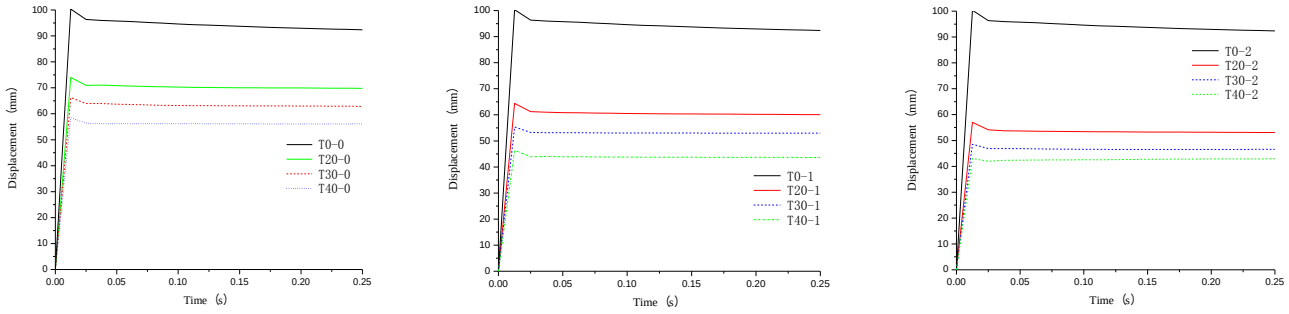

(a) V_f 0% (b) V_f 1% (c) V_f 2%

Fig. 12 Comparison of the displacement versus time curve for different influence considerations

rehabilitation layer thickness, the maximum dynamic deformation of the vehicle impact on the parapet decreases gradually. When the fiber volume fraction is 0%, the parapets of 20 mm, 30 mm, 40 mm thickness of UHPCC rehabilitation layer under the vehicle impact are compared to original parapets that reached the threshold value of the rebars corrosion rate, and the maximum dynamic deformation decreases by 26.2%, 34%, 41.7%; when the fiber volume fraction is 1%, the parapets that used UHPCC 20 mm, 30 mm, 40 mm rehabilitation layer thickness under the vehicle impact are compared to original parapets that reach the threshold value of rebars corrosion rate, the maximum dynamic deformation decreases by 35.8%, 44.9%, 53.3%, respectively; when the fiber volume fraction

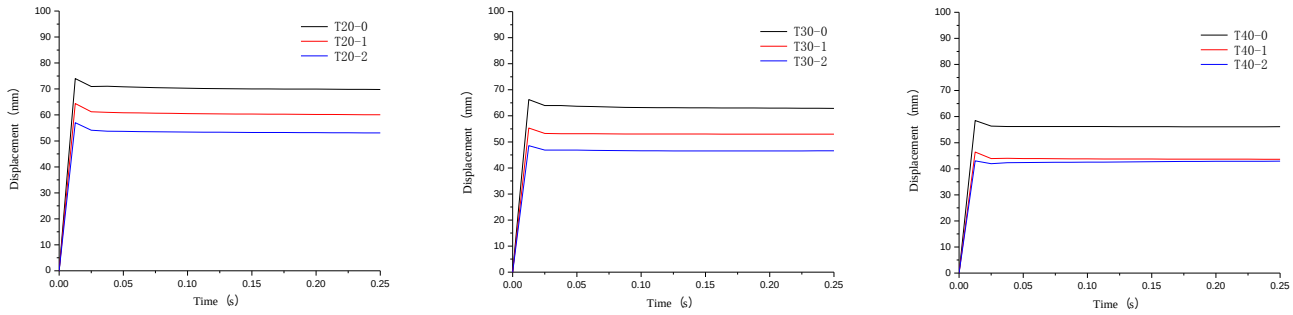

(a) T20 (b) T30 (c) T40

Fig. 13 Comparison of displacement versus time curves for different influence considerations

Table 12 Numerical results of NC parapets rehabilitated by UHPCC for different fiber volume fraction

Name	UT (mm)	Fiber volume fraction (%)	Impact load (kN)	Deformation (mm)	Anti-collision level
T20-0		0	1097	74.01	B
T20-1	20	1	1159	64.4	B
T20-2		2	1209	57.04	B
T30-0		0	1160	66.2	B
T30-1	30	1	1215	55.3	B
T30-2		2	1244	48.56	B
T40-0		0	1192	58.5	B
T40-1	40	1	1246	46.9	B
T40-2		2	1260	43.04	B

is 2%, the parapet that used UHPCC 20 mm, 30 mm, 40 mm rehabilitation layer thickness under the vehicle impact are compared to the above original parapets, the maximum dynamic deformation decreases by 43.2%, 51.6%, 57.1%, respectively.

4.3 Influence of fiber volume fraction

For different fiber volume fraction, the peak impact load and the maximum dynamic deformation of the parapets rehabilitated by UHPCC precast element are shown in Table 12 and Fig. 13.

The numerical results of the peak impact load are compared to show that when the thickness of the UHPCC rehabilitation layer is certain, the peak impact load of parapets increases gradually with the increase of fiber volume fraction. And the maximum dynamic deformation increases gradually. When the thickness of the UHPCC rehabilitation layer is 20 mm, the maximum dynamic deformation of parapets rehabilitated by UHPCC of 0%, 1%, 2% fiber volume fraction decreases by 26.3%, 35.9%, 43.2% respectively; When the thickness of the UHPCC rehabilitation layer is 30 mm, the maximum dynamic deformation of parapets rehabilitated by UHPCC of 0%, 1%, 2% fiber volume fraction decreases by 34.1%, 44.9%, 51.6%; When the thickness of the UHPCC rehabilitation layer is 40 mm, the maximum dynamic deformation of parapets rehabilitated by UHPCC of 0%, 1%, 2% fiber volume fraction decreases by 41.7%, 53.3%, 57.1%.

Table 13 Numerical results of parapets for different impact speeds

Name	Impact speeds (km/h)	Impact load (kN)	Deformation (mm)	Anti-collision level
NC-M1V1θ2	100	654	73	B
NC-M1V2θ2	80	541	37.5	B
NC-M1V3θ2	60	350	19.87	B
M1V1θ2	100	840	38	B
M1V2θ2	80	784	15.1	B
M1V3θ2	60	695	11	B

4.4 Influence of impact speeds

For different impact speeds, the peak impact load and the maximum dynamic deformation of the parapet rehabilitated by UHPCC are shown in Table 13.

The analysis process shows that secondarycollision time of the parapet rehabilitated by UHPCC expands. It can be found that the parapet can dissipate more energy by UHPCC rehabilitation, which can effectively absorb the vehicle kinetic energy and buffer the vehicle collision strength. However, in order to avoid crew casualties accident and reduce property loss, the parapet should not absorb too much energy by UHPCC rehabilitation, namely smaller parapets stiffness is better. Therefore, the rehabilitation and design of parapets also need to be further optimized.

According to Table 13, with the decrease of impact speeds, the maximum dynamic deformation of the parapet rehabilitated by UHPCC decreases gradually, and the change law of the maximum dynamic deformation is same as the original parapet. Compare to original parapets, the maximum dynamic deformation of the parapet rehabilitated by UHPCC decreases by 47.9%, 59.7%, 44.6% when initial speed is 100 km/h, 80 km/h, 60 km/h, respectively.

4.5 Influence of impact angles

The peak impact load results of Table 14 show that when the vehicle of 1.5 t impacts the parapet by the impact

Table 14 Numerical results of parapets for different impact angles

Name	Impact angles (°)	Impact load (kN)	Deformation (mm)	Anti-collision level
NC-M1V2θ1	15	339	15.6	B
NC-M1V2θ2	20	541	37.5	B
NC-M1V2θ3	25	720	64	B
M1V2θ1	15	584	8.3	B
M1V2θ2	20	784	15.1	B
M1V2θ3	25	980	44.7	B
NC-M2V3θ1	15	481	43	B
NC-M2V3θ2	20	523	109	A
NC-M2V3θ3	25	790	162	A
M2V3θ1	15	636	31.8	B
M2V3θ2	20	943	76	A
M2V3θ3	25	1209	126	A
M3V3θ1	15	725	65	B
M3V3θ2	20	1015	108	A
M3V3θ3	25	1298	176	SB
M4V3θ1	15	1036	90	A
M4V3θ2	20	1120	129	SB
M4V3θ3	25	1470	151	SA

speed of 80 km/h, with the increase of impact angles, the peak impact load of parapets rehabilitated by UHPCC increases gradually. The change law of the peak impact load is same as that of original parapets, and the peak impact load increases by 72.3%, 44.9%, 36.1%, respectively. Similarly, we can get the same law when the vehicle of 10 t, 14 t, 18 t impact the parapet by the impact speed of 60 km/h, the corresponding peak impact load is also improved.

According to the results of the maximum dynamic deformation in Table 10, the original parapet rehabilitated by UHPCC before and after is the same when the vehicle that quality of 1.5 t and 10 t impact the parapet in different angles. When the vehicle quality exceeds 10 t, the maximum dynamic deformation of parapets rehabilitated by UHPCC increases with impact angles increasing. Compared with original parapets, the maximum dynamic deformation of parapets rehabilitated by UHPCC decreases by 46.8%, 58.7%, 30.2%, respectively when the vehicle of 1.5 t impacts the parapet by the speed of 80 km/h. The maximum dynamic deformation decreases by 26%, 30.3%, 22.2%, respectively when the vehicle of 10t impacts the parapet by the impact speed of 80 km/h.

4.6 Vehicle mass

The impact angle of 20 degrees is considered in this section with the impact speed of 60 km/h and different vehicle mass. According to the results, the peak impact load and the maximum dynamic deformation of the parapet for different vehicle mass are shown in Table 15.

According to the results, with the increase of vehicle mass, the maximum dynamic deformation of the rehabilitated parapet increases gradually. The change law of the maximum dynamic deformationis same as that of original parapets. According to the above data, the maximum dynamic deformation of the parapet rehabilitated by UHPCC decreases by 44.6%, 30.3%, 42.9% compared with original parapets. The maximum dynamic deformation of the original parapet is 109 mm by the results of the vehicle of 10 t. At this time it is greater than the specification requirement of 100 mm, and the maximum dynamic deformation of the parapet rehabilitated by UHPCC is 76 mm, it meets the specification requirement. It shows that

Table 15 Numerical results of the parapet for different vehicle mass

Name	Vehicle mass (t)	Impact load (kN)	Deformation (mm)	Anti-collision level
NC-M1V3θ2	1.5	350	19.87	B
NC-M2V3θ2	10	523	109	A
NC-M3V3θ2	14	619	172	A
NC-M4V3θ2	18	752	226	SB
M1V3θ2	1.5	695	11	B
M2V3θ2	10	943	76	A
M3V3θ2	14	1015	108	A
M4V3θ2	18	1120	129	SB

Table 16 The anti-collision performance of parapets under different anti-collision levels

Anti-collision level	Rebar corrosion rate (%)	UT (mm)	Impact load (kN)	Deformation (mm)
B	25	20	750	57
	30	20	1036	79
	35	20	765	90
A	25	20	1054	83
	30	20	989	93.2
	35	20	1009	98
SB	25	20	1135	119
	25	30	1502	138
	25	40	1109	92
	30	20	1076	133
	30	30	1126	118
	30	40	1243	98
	35	20	1125	139
	35	30	1237	121
	35	40	1358	106
SA	25	20	1479	143
	25	30	1502	138
	25	40	1430	101
	30	20	1250	158
	30	30	1320	142
	30	40	1452	123
	35	20	1360	164
	35	40	1520	131

the rehabilitation of UHPCC on parapets enhances the anti-collision performance.

4.7 Analysis of anti-collision levels degradation of rehabilitated parapets

On the basis of the above external factors, the anti-collision levels of parapets are divided and analyzed combining the collision energy range in Table 1.

For the B level parapet, initial conditions are the impact speed of 60 km/h, the impact angle of 15 degrees, the vehicle mass of 10 t; For the A level of parapet, the initial conditions are the impact speed of 60 km/h, the impact angle of 15 degrees, the vehicle mass of 18 t; For the SB level parapet, the initial conditions are the impact speed of 60 km/h, the impact angle of 20 degrees, the vehicle mass of 18 t; For the SA level parapet, the initial conditions are the impact speed of 60 km/h, the impact angle of 25 degrees, the vehicle mass of 18 ton.

Under different anti-collision levels, the anti-collision performance of existing RC parapets rehabilitated with UHPCC under different rebar corrosion rates are shown in Table 16.

From Table 13, when the rebar corrosion rate is not more than 35%, B and A levels parapets rehabilitated with 20 mm UHPCC layer meet the requirement of the crashworthiness; When the rebar corrosion rate is not more than 30%, the SB levels parapets rehabilitated with 40 mm UHPCC layer meet the requirement of the crashworthiness, but when the rebar corrosion rate is more than 30%, SB level parapets rehabilitated with 40 mm UHPCC layer cannot meet the requirement and further optimize need to be done; Only when the rebar corrosion rate is less than 25%, the SA level parapets rehabilitated with 40 mm UHPCC layer meet the requirement basically. The anti-collision performance (such as the maximum dynamic deformation and so on) provides a data reference for the anti-collision level determination of parapets in the actual engineering.

5. Conclusions

• Through the vehicle-parapets vertical impact process, the threshold value of corrosion rate of the parapet is 25% and the steel bars corrosion rate influence on peak impact load of anti-collision is not obvious. However, the influence of that on the maximum dynamic deformation is larger.

• When UHPCC rehabilitation layer thickness increases, the peak impact load of parapets increased gradually but the growth rate is smaller. The maximum dynamic deformation decreases gradually. The UHPCC precast element has certain stiffness because of high strength and high modulus of elasticity, and it has a good enhancement effect on the anti-collision performance of the parapet.

• When UHPCC fiber volume fraction increases, the peak impact load of parapets increases gradually, and the maximum dynamic deformation decreases gradually. The analysis results of the peak impact load and the maximum dynamic deformation of the impact position shows that the anti-collision performance are obtained in the degradated parapets rehabilitated by UHPCC.

• With the variety of impact speeds, impact angles and vehicle mass, the change of the peak impact load and the maximum dynamic deformation is same before and after the rehabilitation. Compared with the original parapet, the maximum dynamic deformation significantly reduces after UHPCC rehabilitated parapets. It enhances the anti-collision performance of the parapet, and the parapet rehabilitated by UHPCC lowers restrictions on the vehicle mass.

• For the B and A level parapets, when the rebar corrosion rate is not more than 35%, These parapets rehabilitated with 20 mm UHPCC layer meet the requirement of the anti-collision performance; When the rebar corrosion rate is not more than 30%, the SB level parapets rehabilitated with 40 mm UHPCC layer meet the requirement of the anti-collision performance, but when the rebar corrosion rate is more than 30%, further optimization need to done so that the SB level parapet meet the anti-collision performance requirement; Only when the rebar corrosion rate is less than 25%, the SA level parapets rehabilitated with 40 mm UHPCC layer meet the anti-collision performance requirements basically.

Acknowledgements

The authors would like to thank the Heilongjiang Province Natural Science Fund (E2015014) for providing funding to this project, the National Natural Science Foundation of China (51008088) (51678196), the Fundamental Research Funds for the Central Universities (Grant No. HIT. NSRIF. 2013112), Harbin City Science and Technology Innovation Talents Special Funds (2011RFLXG014), and the National Key Technology Research and Development Program of China under Grant No. 2011BAJ10B0102 for the supporting the authors' work described herein.

References

Almusallam, A.A. (2001), "Effect of corrosion on the properties of reforcing steel bars", *Constr. Build. Mater.*, **15**(8), 361-368.

Bastien Masse, M. and Bruehwiler, E. (2014), "Ultra high performance fiber reinforced concrete for strengthening and protecting bridge deck slabs", *Bridge Mainten. Safety Manage. Life Extens.*, EPFL-CONF-202494, 2176-2182.

Benjamin, A. and Graybeal, B.A. (2006), "Structural behavior of ultra-high performance concrete prestressed I-girders", FHWA-HRT-06-115.

Brühwiler, E. and Denarie, E. (2008),"Rehabilitation of concrete structures using ultra-high performance fibre reinforced concrete", *Proceedings of the Second International Symposium on Ultra High Performance Concrete*, Kassel, Germany.

Bruhwiler, E. and Denarie, E. (2013), "Rehabilitation and strengthening of concrete structures using ultra-high performance fibre reinforced concrete", *Struct. Eng. Int.*, **23**(4), 450-457.

Brühwiler, E. and Denarie, E. (2013), "Stahl-UHFB-stahlbeton verbundbauweise zur Verstärkung von bestehenden Stahlbetonbauteilen mit Ultra-hochleistungs-faserbeton (UHFB)", *Beton-undStahlbetonbau*, **108**(4), 216-226.

Charron, J.P., Niamba, E. and Massicotte, B. (2011), "Precast

bridge parapets in ultra high performance fiber-reinforced concrete", *Design. Build.*, UHPFRC, 391-404.
Duchesneau, F., Charron, J.P. and Massicotte, B. (2011), "Monolithic and hybrid precast bridge parapets in high and ultra-high performance fibre reinforced concretes", *Can. J. Civil Eng.*, **38**(8), 859-869.
Dugat, J., Roux, N. and Bernier, G. (1996), "Mechanical properties of reactive powder concretes", *Mater. Struct.*, **29**(188), 233-240.
Habel, K. and Gauvreau, P. (2009), "Behavior of reinforced and posttensioned concrete members with a UHPFRC overlay under impact loading", *J. Struct. Eng.*, **135**(3), 292-300.
Industry Recommended Standard of the R.P.C. (2006), *Guidelines for Design of Highway Safety Facilities*, Ministry of Transport of the P.R.C., JTG/TD812006.
Moreillon, L. and Menetrey, P. (2013), "Rehabilitation and strengthening of existing RC structures with UHPFRC: Various applications", *Proceedings of the International Symposium on Ultra-High Performance Fibre-Reinforced Concrete*, RILEM Publication S.A.R.L., RILEM-fib-AFGC, France.
National Standard of the P.R.C. (1994), *Code for Design of Highway Traffic Safety Facilities*, Ministry of Transport of the P.R.C., JTJ074-94.
National Standard of the P.R.C. (2004), *The Evaluation Specification for Highway Safety Barriers*, Ministry of Transport of the P.R.C., JTG/T F83-01-2004.
National Standard of the P.R.C. (2010), *Code for Design of Concrete Structures*, China Planning Press, Beijing, GB50010-2010.
Oesterlee, C., Denarie, E. and Bruhwiler, E. (2007), "UHPFRC protection layer on the crash barrier walls of a bridge", *Adv. Constr. Mater.*, Springer Berlin Heidelberg, 203-210.
Prem, P.R., Murthy, A.R., Ramesh, G., Bharatkumar, B.H. and Lyer, N.R. (2015), "Flexural behavior of damaged RC beams strengthened with ultra high performance concrete", *Adv. Struct. Eng.*, 2057-2069.
Schmidt, C., Riedl, S., Geisenhanslüke, C. and Schmidt, M. (2008), "Strengthening and rehabilitation of pavements applying thin layers of reinforced ultra-high performance concrete (UHPC-white topping)", *Proceedings of the Second International Symposium on Ultra-High Performance Concrete*, Kassel, Germany.
Tai, Y.G. (2010), "Simulation and experiment of crashworthiness for combined bridge guardrail", *J. Traffic Transport. Eng.*, **10**(1), 94-100.
Wang, J.Q. (2003), "Experiment study and analysis on the mechanical properties of corroded reinforcing bars in the atmospheric environment", *J. Xuzhou Inst. Architect. Technol.*, **3**(3), 25-27.
Wang, Y., An, M., Yu, Z., Su, J. and Li, Z. (2013), "Research on the mechanical properties of reactive powder concrete: A review", *Concrete*, **290**(12), 21-26.
Wu, X.G. Yang, J. and Mpalla, I.B. (2013), "Preliminary design and structural responses of typical hybrid wind tower made of ultra high performance cementitious composites", *Struct. Eng. Mech.*, **48**(6), 791-807.
Wu, X.G., Hu, Q., Zou, R.F., Zhao, X.Y. and Yu, Q. (2014), "Structural behaviors of sustainable hybrid columns under compression and flexure", *Struct. Eng. Mech.*, **52**(5), 857-873.
Wu, X.G., Zhao, X.Y. and Han, S.M. (2012), "Structural analysis of circular UHPCC form for hybrid pier under construction loads", *Steel Compos. Struct.*, **12**(2), 167-181.
Yang, Z.H. (2006), "Study on tension mechanical performance of reactive powder concrete in different steel fiber volume fractions", M.S. Dissertation, Beijing Jiaotong University, Beijing.
Zhang, P.S., Lu, M. and Li, X.Y. (1995), "Mechanical property of rustiness reinforcement steel", *Industr. Constr.*, **25**(9), 41-44.
Zhang, P.S., Shang, D.F. and Gu, X.L. (2006), "Stress-strain relationship of corroded steel bars", *J. Tongji Univ.*, **34**(5), 586-592.

CC